Mol. Cells *27*, 591-599, May 31, 2009
DOI/10.1007/s10059-009-0073-4

Molecules and Cells

A Role for Leu247 Residue within Transmembrane Domain 2 in Ginsenoside-Mediated α7 Nicotinic Acetylcholine Receptor Regulation

Byung-Hwan Lee[1,9], Sun-Hye Choi[1,9], Mi Kyung Pyo[1], Tae-Joon Shin[1], Sung-Hee Hwang[1], Bo-Ra Kim[1], Sang-MoK Lee[1], Jun-Ho Lee[2], Joon-Hee Lee[3], Hui Sun Lee[4], Han Choe[4], Kyou-Hoon Han[5], Hyoung-Chun Kim[6], Hyewhon Rhim[7], Joon-Hwan Yong[8], and Seung-Yeol Nah[1,*]

Nicotinic acetylcholine receptors (nAChRs) play important roles in nervous system functions and are involved in a variety of diseases. We previously demonstrated that ginsenosides, the active ingredients of *Panax* ginseng, inhibit subsets of nAChR channel currents, but not α7, expressed in *Xenopus laevis* oocytes. Mutation of the highly conserved Leu247 to Thr247 in the transmembrane domain 2 (TM2) channel pore region of α7 nAChR induces alterations in channel gating properties and converts α7 nAChR antagonists into agonists. In the present study, we assessed how point mutations in the Leu247 residue leading to various amino acids affect 20(*S*)-ginsenoside Rg_3 (Rg_3) activity against the α7 nAChR. Mutation of L247 to L247A, L247D, L247E, L247I, L247S, and L247T, but not L247K, rendered mutant receptors sensitive to Rg_3. We further characterized Rg_3 regulation of L247T receptors. We found that Rg_3 inhibition of mutant α7 nAChR channel currents was reversible and concentration-dependent. Rg_3 inhibition was strongly voltage-dependent and noncompetitive manner. These results indicate that the interaction between Rg_3 and mutant receptors might differ from its interaction with the wild-type receptor. To identify differences in Rg_3 interactions between wild-type and L247T receptors, we utilized docked modeling. This modeling revealed that Rg_3 forms hydrogen bonds with amino acids, such as Ser240 of subunit I and Thr244 of subunit II and V at the channel pore, whereas Rg_3 localizes at the interface of the two wild-type receptor subunits. These results indicate that mutation of Leu247 to Thr247 induces conformational changes in the wild-type receptor and provides a binding pocket for Rg_3 at the channel pore.

INTRODUCTION

Nicotinic acetylcholine receptors (nAChRs) are members of the Cys-loop family of ligand-gated ion channels, which also includes 5-HT_3, $GABA_A$, and glycine receptors (Jensen et al., 2005). There are muscular and neuronal forms of nAChRs. The muscular nAChR consists of $\alpha_1\beta_1\delta\varepsilon$ subunits, whereas neuronal consist of α alone or α and β subunit combinations. Neuronal nAChR α ($\alpha_{2\text{-}10}$) and β ($\beta_{2\text{-}4}$) subunits have been identified (Le Novere and Changeux, 1995; Nashmi and Lester, 2006). The nAChRs containing $\alpha_{2\text{-}6}$ subunits are usually expressed as heteromers in combination with $\beta_{2\text{-}4}$ subunits (Boulter et al., 1986; 1987; Karlin, 2002), and are found in the central and peripheral nervous systems (Gotti and Clementi, 2004). In contrast, the α_7 and α_9 subunits can form homomeric receptors (Couturier et al., 1990; Elgoyhen et al., 1994; Gotti et al., 1994; Karlin, 2002). Homomeric α7 nAChRs are the major binding site for α-bungarotoxin in the mammalian central nervous system and are predominantly expressed in cortical and limbic areas (Gotti et al., 2000). Many lines of evidence have shown that single point mutation in the highly conserved Leu247 to Thr247 in transmembrane domain 2 (TM2), which forms the channel pore region, creates gain-of-function alterations (i.e., slower desensitization, increased acetylcholine affinity, and a linear current-voltage relationship) and alters pharmacological properties (i.e., conversion of various α7 AChR antagonists into agonists) (Bertrand et al., 1992; Palma et al., 1996; Revah et al., 1991). Thus, the L247 residue of α7 AChR could be a useful target for the study of α7 AChR-related pharmacology (i.e., drug developments) and channel gating of AChR (Lyford et al., 2003).

[1]Ginsentology Research Laboratory and Department of Physiology, College of Veterinary Medicine, Konkuk University, Seoul 143-701, Korea, [2]Department of Physiology, College of Oriental Medicine, Kyung-Hee University, Seoul 130-701, Korea, [3]Department of Physical Therapy, Daebul University, Jeonnam 526-702, Korea, [4]Department of Physiology and Research Institute for Biomacromolecules, University of Ulsan, College of Medicine, Seoul 138-736, Korea, [5]Protein Analysis and Design Section, Molecular Cancer Research Center, Korea Research Institute of Bioscience and Biotechnology, Daejeon 305-806, Korea, [6]Neuropsychopharmacology and Toxicology Program, College of Pharmacy, Kangwon National University, Chunchon 200-701, Korea, [7]Life Science Division, Korea Institute of Science and Technology, Seoul 136-791, Korea, [8]Department of Occupational Therapy, Dongnam Health College, Suwon 440-714, Korea, [9]These authors contributed equally to this work.
*Correspondence: synah@konkuk.ac.kr

Received February 20, 2009; revised March 18, 2009; accepted March 19, 2009; published online May 15, 2009

Keywords: ginsenoside Rg_3, interaction sites, mutant α7 nAChR, *Panax* ginseng

In previous reports, we have shown that treatment with ginsenosides, the active ingredients of *Panax* ginseng, inhibit acetylcholine-induced peak inward currents (I_{ACh}) of neuronal (α3β2, α3β4, α4β2 and α4β4) and muscle-type heteromeric ($\alpha_1\beta_1\delta\varepsilon$) nAChR channels expressed in *Xenopus laevis* oocytes. Inhibition of I_{ACh} by ginsenosides is voltage-dependent and noncompetitive (Choi et al., 2002; Sala et al., 2002). As described above, α7 nACh and 5-HT_{3A} receptors are members of the same family and are both homomeric ligand-gated ion channels. Furthermore, these receptors share many homologous amino acid sequences in TM2 (Fig. 1B). We have shown that ginsenosides, including Rg_3, inhibit 5-HT-mediated ion currents in *Xenopus* oocytes expressing 5-HT_{3A} receptors. Moreover, mutation F292A in TM2 of the homomeric 5-HT_{3A} receptor abolished Rg_3-induced inhibition of peak $I_{5\text{-}HT}$, showing a possibility that ginsenoside-induced ligand-gated cation channel regulation is achieved via interactions with amino acids residing in the channel pore (Lee et al., 2007). However, the same Rg_3 effect on wild-type α7 nAChR channel activity is not observed (Choi et al., 2002; Sala et al., 2002).

Therefore, in the present study we asked whether mutation of Leu247 to various other amino acid residues induce changes in the receptor sensitivity to Rg_3. Finding this to be true, we further characterized Rg_3-mediated mutant α7 nAChR regulation and identified potential Rg_3 interaction sites with the mutant receptor using three-dimensional modeling techniques. In this report, we found that Rg_3 inhibited L247A, L247D, L247E, L247I, L247S and L247T, but not L247K and wild-type α7 nAChR channel currents. The docked modeling studies using wild-type and L247T mutant receptors showed that mutation of Leu247 to Thr247 induces conformational changes in the wild-type receptor and also alters the Rg_3 binding location from the interface of two wild-type subunits to channel pore regions of the mutant receptor. We also observed that Rg_3 interacts with Thr244 and Ser240 in the central pore formed by TM2 of L247T α7 subunits through the formation of hydrogen bonds. Together, these results indicate that the Leu247 residue might play an important role in Rg_3-induced inhibition of I_{ACh} through the α7 nAChR when mutated and that inhibition of I_{ACh} in L247T receptors by Rg_3 is achieved through interactions with channel pore amino acids.

MATERIALS AND METHODS

Materials

20(*S*)-Ginsenoside Rg_3 (Rg_3) was purchase from LKT LABS (USA). Chick wild-type α7 nAChR cDNA was kindly provided by Dr. M. Ballivet (Univ. of Geneva, Switzerland). All other reagents were purchased from Sigma-Aldrich (USA).

Preparation of *Xenopus laevis* oocytes and microinjection

X. laevis frogs were purchased from Xenopus I (Ann Arbor, USA). Animal care and handling were in accordance with the highest standards of institutional guidelines. To isolate oocytes, frogs were anesthetized with an aerated solution of 3-amino benzoic acid ethyl ester, and the ovarian follicles were removed. The oocytes were separated with collagenase followed by agitation for 2 h in Ca^{2+}-free medium containing 82.5 mM NaCl, 2 mM KCl, 1 mM $MgCl_2$, 5 mM HEPES, 2.5 mM sodium pyruvate, 100 units/ml penicillin, and 100 μg/ml streptomycin. Stage V-VI oocytes were collected and stored in ND96 medium (96 mM NaCl, 2 mM KCl, 1 mM $MgCl_2$, 1.8 mM $CaCl_2$, and 5 mM HEPES, pH 7.5) supplemented with 0.5 mM theophylline and 50 μg/ml gentamicin. The oocyte-containing solution was maintained at 18°C with continuous gentle shaking and was replaced daily. Electrophysiological experiments were performed five to six days following oocyte isolation, during which chemicals were applied to the bath. For α7 nAChR experiments, α7 nAChR-encoding cRNAs (40 nl) were injected into the animal or vegetal pole of each oocyte 1 day after isolation using a 10-μl microdispenser (VWR Scientific, USA) fitted with a tapered

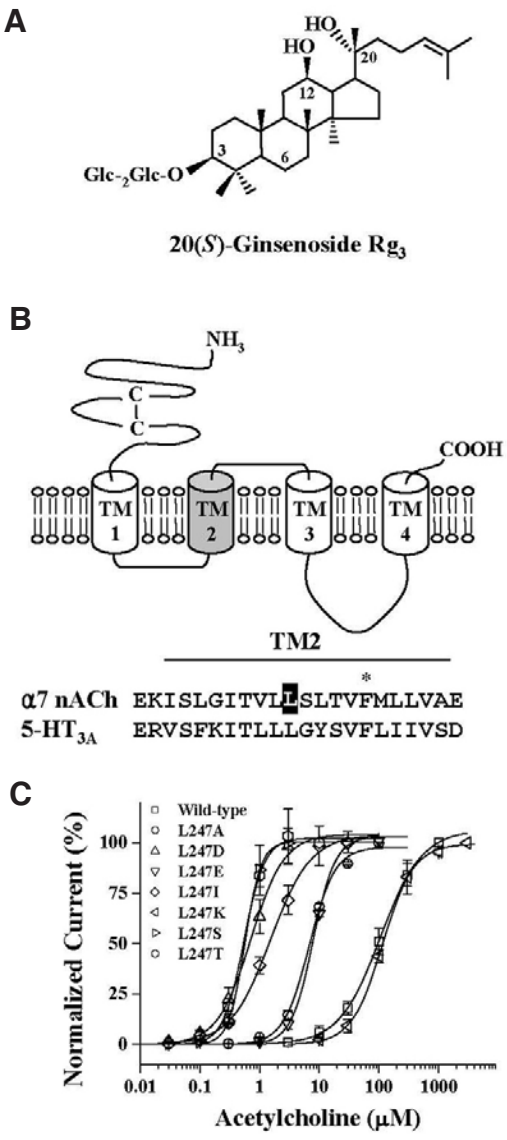

Fig. 1. Structure of 20(*S*)-ginsenoside Rg_3 (Rg_3), the primary amino acid sequences of the channel-lining regions (TM2) of chick α7 nACh and mouse 5-HT_{3A} receptors, and concentration-response curves of acetylcholine in wild-type and α7 mutant receptors. (A) Structure of 20(*S*)-ginsenoside Rg_3. Glc, glucopyranoside. Subscripts indicate the carbon in the glucose ring that links the two carbohydrates. (B) Partial amino acid sequences of the TM2 region of the cloned chick α7 nACh and mouse 5-HT_{3A} receptors. The dark box shown on the wild-type α7 nAChR receptor indicates amino acid residues that were mutated in the present study. (C) Concentration-response curves of the acetylcholine-induced current in wild-type and various mutant receptors. Additional EC_{50} and Hill coefficient values for the various mutants are presented in Table 1. Each point represents the means ± S.E.M. (n = 9-12/group).

glass pipette tip (15-20 μm in diameter) (Lee et al., 2005).

Site-directed mutagenesis of chick α7 nAChR and *in vitro* transcription of α7 nAChR cDNAs

Single amino acid substitutions were made using the QuikChange XL site-directed mutagenesis kit (Stratagene, USA) along with *Pyrococcus furiosus* DNA polymerase and sense and antisense primers encoding the desired mutations. Overlap extension of the target domain by sequential polymerase chain reaction (PCR) was carried out according to the manufacturer's protocol. The final PCR products were transformed into *Escherichia coli* strain DH5α, screened by PCR, and confirmed by sequencing of the target regions. The mutant DNA constructs were linearized at the 3′ ends by digestion with SphI, and run-off transcripts were prepared using the methylated cap analog $m^7G(5')ppp(5')G$. The cRNAs were prepared using an mMessage mMachine transcription kit (Ambion, USA) with T7 RNA polymerase. The absence of degraded RNA was confirmed by denaturing agarose gel electrophoresis followed by ethidium bromide staining. Recombinant plasmids containing α7 nAChR cDNA inserts were linearized by digestion with the appropriate restriction enzymes, and cRNAs were obtained using the mMessage mMachine *in vitro* transcription kit with T7 polymerase. The final cRNA products were resuspended at a concentration of 1 μg/μl in RNase-free water and stored at -80°C (Lee et al., 2005).

Data recording

A custom-made Plexiglas net chamber was used for two-electrode voltage-clamp recordings, as previously reported (Lee et al., 2005). A single oocyte was constantly superfused with ND96 medium in the absence or presence of acetylcholine or Rg_3 during recording. The microelectrodes were filled with 3 M KCl and had a resistance of 0.2-0.7 MΩ. Two-electrode voltage-clamp recordings were obtained at room temperature using an Oocyte Clamp (OC-725C, Warner Instrument) and digitized using Digidata 1200A (Molecular Devices, USA). Stimulation and data acquisition were controlled using pClamp 8 software (Molecular Devices). For most electrophysiological experiments, the oocytes were clamped at a holding potential of -80 mV, and 300-ms voltage steps were applied from -100 to +50 mV to assess the current and voltage relationship. Linear leak and capacitance currents were corrected by means of the leak subtraction procedure. Since α7 nAChRs have a high relative permeability to Ca^{2+} (Castro and Albuquerque, 1995; Seguela et al., 1993), oocytes were incubated in 100 μM BAPTA-AM for 4 h before recording to avoid α7 nAChR-mediated endogenous Ca^{2+}-activated Cl^- currents.

Homology modeling

A homology model of the chick α7 AChR was constructed on the 4 Å structure of the membrane-associated *Torpedo* acetylcholine receptor (PDB code 2BG9) (Unwin, 2005) using the homology modeling program MODELLER 9v2 (Sali and Blundell, 1993). Transmembrane domains were predicted using TMHMM server v2.0 (Krogh et al., 2001), and the secondary structures were predicted using the PSIPRED server (Bryson et al., 2005). Sequence alignment between the chick α7 AChR channel and the *Torpedo* acetylcholine receptor channel was carried out manually paying special attention to the alignment of the predicted transmembrane domains. A stretch of amino acids from Lys303 to Ala411 in the chick α7 nAChR was not included in the modeling because the corresponding regions were missing in the PDB file. The excluded 109 amino acids form the intracellular disordered loop between the M3 and M4 transmembrane domains and are presumed to be unimportant for Rg_3 binding. Hydrogen atoms were added to the homology model and then the structure was energy-minimized using Sybyl v7.0 (Tripos Inc., USA). The minimization procedure was implemented by Powell minimization algorithm using the derivative convergence criterion of 0.05 kcal/Å-mol. Tripos force field and Gasteiger-Huckel charge model were employed for the energy-minimization. The same strategies were used to generate a homology model of the L247T mutant receptor.

Virtual docking of Rg_3 to wild-type and L247T α7 nAChRs

The structure of (*S*)-Rg_3 was constructed using Chemdraw ultra 8.0 (Cambridgesoft, USA), and converted to a 3-dimensional model and energy minimized using Chem3D ultra 8.0 (Cambridgesoft, USA), followed by one round of energy minimization using the Sybyl forcefield. Virtual dockings of (*S*)-Rg_3 to the homology model of wild-type α7 AChR and L247T mutant channels were performed using GOLD v3.0 (The Cambridge Crystallographic Data Centre, UK), a program that uses stochastic genetic algorithms for conformational searches (Verdongk et al., 2003). The docking by GOLD was performed under the standard default settings mode allowing full ligand flexibility and keeping the protein rigid. The L247 or T247 residues in each of the five subunits were designated as the active site residues, and the active radius was set to 10 Å from the active site residues. Docked models displaying the best GOLD scores (best-fit docking results) were selected for final complex structural analysis. The poseview computer program (Stierand et al., 2006) was used to investigate the interactions of the protriptyline molecule with the HERG channel. All structural figures were prepared using PyMol v0.98 (DeLano Scientific LLC, USA).

Data analysis

To obtain the concentration-response curve for the effect of Rg_3 on the inward peak I_{ACh} mediated by the α7 AChR, the I_{ACh} peak was plotted at different concentrations of Rg_3 and the Origin software (OriginLab Corp., USA) was used to fit the plot to the Hill equation: $I/I_{max} = 1/[1 + (IC_{50}/[A])^{nH}]$, where I_{max} is maximal current obtained from each EC_{50} value of acetylcholine in mutant receptors as shown in Table 1. IC_{50} is the concentration of Rg_3 required to decrease the response by 50%. [*A*] is concentration of Rg_3 and nH is the Hill coefficient. All values are presented as means ± S.E.M. The differences between means of control and treatment data were determined using the unpaired Student's *t*-test or one-way ANOVA. A value of $p < 0.05$ was considered statistically significant.

RESULTS

Effects of Rg_3 on wild-type and Leu247 mutant nAChRs

In previous reports, we showed that ginsenosides inhibit several subtypes of heteromeric, but not homomeric, α7 nAChRs (Choi et al., 2002; Sala et al., 2002). Likewise, in the present study we found no inhibitory effect of Rg_3 on I_{ACh} at concentrations up to 300 μM for the wild-type α7 nAChR expressed in *Xenopus* oocytes (Fig. 2A). We have recently shown that the inhibitory effect of Rg_3 on 5-HT_{3A} receptor channel currents was abolished by mutation of Phe292 to Ala292 (F292-F292A) in TM2 (Lee et al., 2007). We first examined the possibility that Rg_3 affects I_{ACh} in F252A mutant receptor, since this amino acid is homologous to that present in the homomeric 5-HT_{3A} receptor (Fig. 1B, *asterisk*). However, Rg_3 did not affect the activity of this mutant channels (data not shown). These results together with previous finding suggest that although the amino acid sequences of the TM2 domain are very similar to that of the 5-

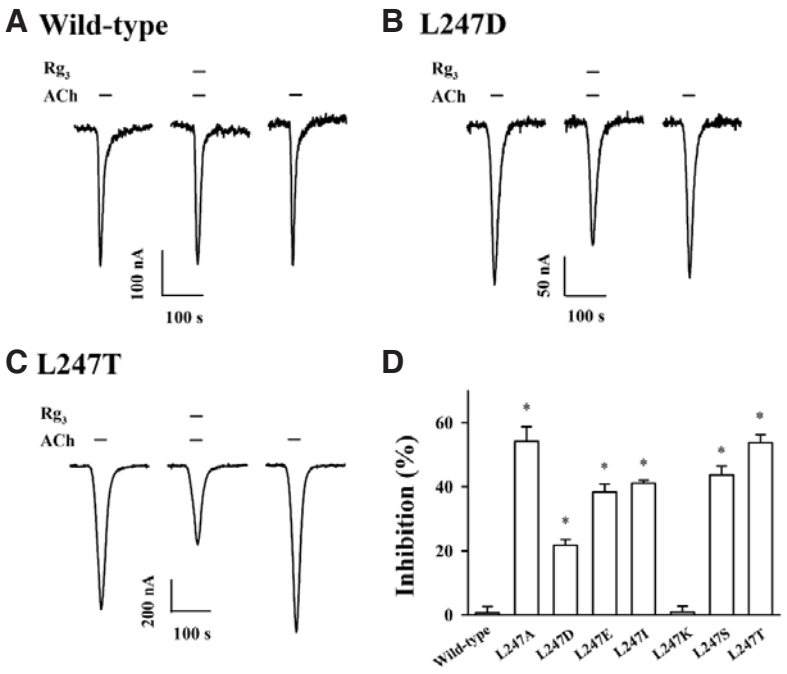

Fig. 2. Effect of Rg_3 on I_{ACh} in oocytes expressing wild-type or one of the various mutant α7 nAChRs. (A) Acetylcholine (100 μM) was applied first, followed by co-application of acetylcholine and Rg_3. Co-application of 100 μM Rg_3 with acetylcholine had no effect on I_{ACh}. (B) Acetylcholine (0.7 μM) was applied first, followed by co-application of acetylcholine and Rg_3. Co-application of 100 μM Rg_3 with acetylcholine inhibited I_{ACh} in L247D receptors. (C) Acetylcholine (0.5 μM) was applied first, followed by co-application of acetylcholine and Rg_3. Co-application of 100 μM Rg_3 with acetylcholine also inhibited I_{ACh} in L247T receptors. (D) Summary of the current inhibition, presented as percent inhibition, induced in wild-type and various receptors mutated at the Leu247 residue by Rg_3. The resting membrane potentials of the oocytes were about -35 mV, and they were voltage-clamped at a holding potential of -80 mV prior to drug application. Traces are representative of six separate oocytes from three different batches of frogs. Each point represents the means ± S.E.M. (n = 9-12/group).

HT_{3A} receptor, the mechanism of ginsenoside action on α7 nAChR might differ from those of heteromeric nAChRs and the wild-type 5-HT_{3A} receptor.

Previous reports have shown that mutation of Leu247 to L247T in TM2 of the α7 nAChR induces alterations of various receptor channel properties as well as receptor pharmacology (Bertrand et al., 1992; Palma et al., 1996; Revah et al., 1991). We also constructed L247T receptor and first examined the effects of acetylcholine on mutant receptor channel activation. We found that application of acetylcholine to these mutant receptors, excluding the L247K mutant receptor, greatly increased I_{ACh}. In addition, mutant receptors displayed a significant leftward shift in the concentration-response curve for acetylcholine, indicating a reduced EC_{50} value compared to the wild-type receptor and increased acetylcholine potency for the mutant receptors (Palma et al., 1996; Revah et al., 1991) (Fig. 1C; Table 1). We next examined the effect of Rg_3 on the I_{ACh} of the mutant receptors. Surprisingly, we found that Rg_3 exhibited inhibitory effects on L247T α7 nAChR channel currents despite the increased affinity of acetylcholine for the mutant receptors (Fig. 2C). In addition, we examined the effect of Rg_3 after replacement of the Leu247 residue with other amino acids. We found that mutation of Leu247 to L247A, L247D, L247E, L247I, or L247S, but not L247K, sensitized the receptor to Rg_3. The order of Rg_3-mediated % inhibition of I_{ACh} in mutant nAChRs was: L247A = L247T > L247S > L247I = L247E > L247D. Rg_3 had no effect on mutant L247K or wild-type receptor channel activity (Fig. 2D). We examined the effects of Rg_3 on I_{ACh} in mutant receptors such as L246T and S248A, which are amino acid residues adjacent to L247T, but found no effect of Rg_3 on these mutants (data not shown). In addition, we also examined the effects of Rg_3 on I_{ACh} in double mutant receptor such as L247T-F292A to know whether this double mutation abolishes the inhibitory effect of Rg_3 on I_{ACh} observed in L247T α7 receptor but found that Rg_3 still maintained the inhibition on I_{ACh} in double mutant receptors as much as in L247T receptor (data not shown). These results indicate that Rg_3-mediated I_{Ach} regulation depends upon the particular residue at 247 when it is mutated with other amino acids.

Table 1. Effects of acetylcholine on wild-type and various mutant α7 nAChRs expressed in *Xenopus* oocytes

	EC_{50}	*n*H
Wild-type	105.6 ± 2.4	1.3 ± 0.0
L247A	6.8 ± 0.5*	2.0 ± 0.2
L247D	0.71 ± 0.06*	1.6 ± 0.2
L247E	7.9 ± 0.25*	2.3 ± 0.2
L247I	1.5 ± 0.10*	1.3 ± 0.1
L247K	115.4 ± 3.1	1.7 ± 0.1
L247S	0.56 ± 0.01*	3.2 ± 0.1*
L247T	0.54 ± 0.02*	2.5 ± 0.2*

Values represent means ± S.E.M. (n = 9-12/group). Currents were elicited at a holding potential of -80 mV. EC_{50} (μM) and Hill coefficient values were determined as described in the Experimental procedures.
*$p < 0.005$, compared with wild-type α7 nAChRs.

Concentration-dependent effect of Rg_3 on I_{ACh} in oocytes expressing various mutant α7 nicotinic acetylcholine receptors

Co-application of Rg_3 and acetylcholine inhibited I_{ACh} in a concentration-dependent manner in oocytes expressing various mutant α7 nAChRs (Fig. 3; Table 2). We used the EC_{50} value obtained from each mutant receptor as the concentration of acetylcholine used in these experiments (Table 1). The IC_{50} values of Rg_3 were 33.1 ± 1.3, 56.3 ± 23.6, 57.4 ± 9.9, 81.9 ± 23.2, 66.0 ± 22.4, and 30.4 ± 1.8 μM in oocytes expressing L247A, L247D, L247E, L247I, L247S, and L247T α7 nicotinic acetylcholine receptors, respectively (n = 9-12 from three different frogs). Thus, the order of IC_{50} values was: L247I > L247S > L247D = L247E> L247A > L247T (Fig. 3; Table 2).

Current-voltage relationship and noncompetitive inhibition of L247T α7 nAChRs by Rg_3

We examined L247T receptor current-voltage (*I-V*) relation-

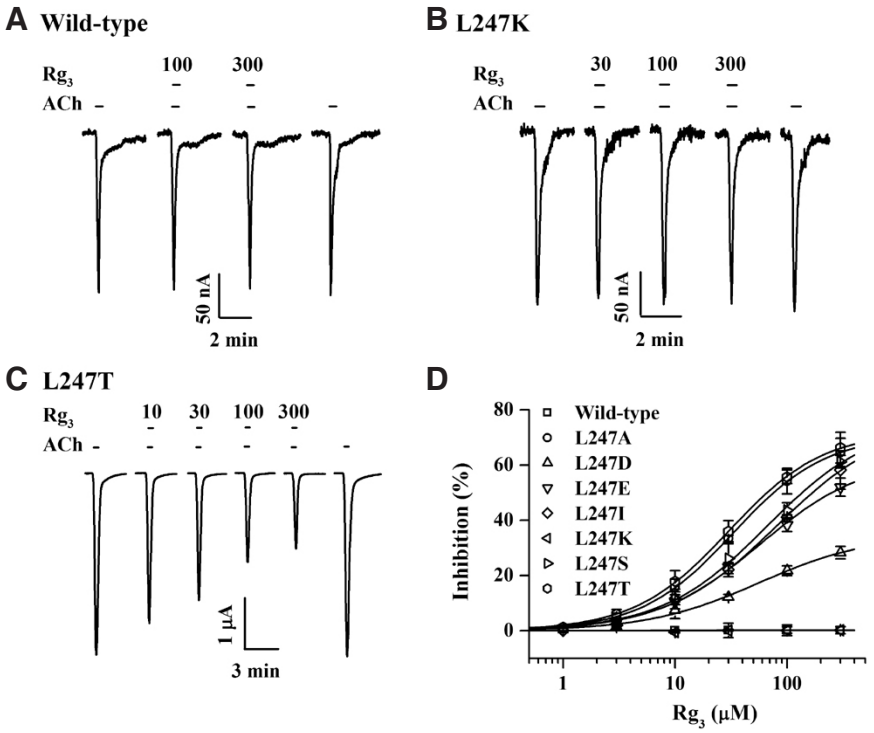

Fig. 3. Concentration-dependent effects of Rg_3 on I_{ACh} in wild-type and various mutant α7 nAChRs. I_{ACh} in oocytes expressing wild-type, L247A, L247D, L247E, L247I, L247K, L247S, or L247T mutant receptors was elicited at a holding potential of -80 mV for the indicated time in the presence of acetylcholine (EC_{50} value of wild-type and each mutant receptor), followed by co-application of the indicated concentrations of acetylcholine together with Rg_3. (A-C) Traces representative of nine separate oocytes from three different frogs. (D) Concentration-response curves showing the effect of Rg_3 on oocytes expressing the wild-type or various mutant receptors. The solid lines were fitted using the Hill equation. Additional IC_{50}, Hill coefficient, and V_{max} values for the various mutants are presented in Table 2 (means ± S.E.M; n = 9-12 oocytes for each point).

Table 2. Effects of Rg_3 on various mutant α7 nAChRs expressed in *Xenopus* oocytes

	IC_{50}	V_{max}	*n*H
L247A	33.1 ± 1.3	70.9 ± 1.1	1.1 ± 0.1
L247D	56.3 ± 9.6	34.8 ± 4.9	0.9 ± 0.2
L247E	57.4 ± 9.9	62.8 ± 3.8	0.9 ± 0.1
L247I	81.9 ± 10.2	76.4 ± 7.8	0.9 ± 0.1
L247K	ND	ND	ND
L247S	66.0 ± 7.4	75.7 ± 9.2	0.9 ± 0.1
L247T	30.3 ± 1.3	72.4 ± 1.1	1.0 ± 0.1

Values represent means ± S.E.M. (n = 8-10/group). Currents were elicited at a holding potential of -80 mV. V_{max} is the maximal inhibition for a given mutant at the highest concentration of Rg_3 and IC_{50} (μM), and Hill coefficient values were determined as described in the experimental procedures. ND is not determined.

ships in the absence or presence of Rg_3. We measured the amplitude of current activated by either acetylcholine alone or acetylcholine plus Rg_3 at an initial holding potential of -80 mV, which was then ramped from -100 to +50 mV over 300 ms. In the absence of acetylcholine, oocytes expressing L247T receptors evoked an inward current of < 0.01 μA at -100 mV and an outward current of ~0.1 μA at +50 mV. In oocytes expressing L247T receptors, acetylcholine treatment evoked a current that reversed at approximately -10 mV, and both the inward and outward currents were inhibited by Rg_3 (Choi et al., 2002). Oocytes expressing L247T mutant channels showed no significant differences in reversal potential for acetylcholine in the absence or presence of Rg_3 (without Rg_3, -10.4 ± 2.5 mV; with Rg_3, -11.5 ± 2.8 mV; $p < 0.5$) (Fig. 4A). To further study the mechanism by which Rg_3 inhibits I_{ACh} in oocytes expressing L247T α7 nAChRs, we analyzed the effect of Rg_3 on I_{ACh} evoked by various acetylcholine concentrations in oocytes expressing L247T α7 nAChRs (Fig. 4B). Co-application of Rg_3 with various concentrations of acetylcholine did not shift the concentration-response curve of acetylcholine to the right (EC_{50} from 0.54 ± 0.02 to 0.59 ± 0.01 μM and Hill coefficient from 2.5 ± 0.2 to 2.2 ± 0.02) in oocytes expressing L247T α7 nAChRs, although Rg_3 significantly inhibited I_{ACh} at concentrations of 1, 3, and 10 μM acetylcholine (*$p < 0.05$, **$p < 0.005$, compared to the absence of Rg_3, n = 8-10 from three different frogs), indicating that Rg_3 reduced I_{ACh} in L247T α7 nAChRs with equal potency, independently of the acetylcholine concentration (n = 9-12 from three different frogs) (Fig. 4B).

Voltage-dependent inhibition of I_{ACh} by Rg_3 in oocytes expressing L247T α7 nAChRs

We next examined whether the inhibitory effect of Rg_3 on I_{ACh} in oocytes expressing L247T α7 nAChRs was dependent on the membrane holding potential. As shown in Fig. 5, although Rg_3 did not exhibit any effects on I_{ACh} in oocytes expressing wild-type α7 nAChRs at different membrane holding potentials, the inhibitory effect of Rg_3 on I_{ACh} in oocytes expressing L247T α7 nAChRs demonstrated a significant dependence (Fig. 5C). Thus, Rg_3 inhibited I_{ACh} by 63.4 ± 2.6, 48.6 ± 2.0, 38.2 ± 3.3, 29.8 ± 5.3 and 18.3 ± 1.2% at -120, -90, -60, -30, and 0 mV holding potentials, respectively, in oocytes expressing L247T α7 nAChRs (*$p < 0.005$, compared to -120 mV membrane holding potential; n = 9-12 from three different frogs). These results indicate that Rg_3 inhibits I_{ACh} in the L247T receptor in a voltage-dependent manner.

Virtual docking of Rg_3 to wild-type and L247T α7 nAChRs

To further examine the possible interactions between Rg_3 and the α7 AChR channel, computational simulations of wild-type and L247T mutant AChR channels were constructed and evaluated. Homology modeling of the channels and virtual docking of Rg_3 to the homology models were performed using the MODELLER and GOLD programs, respectively. Interest-

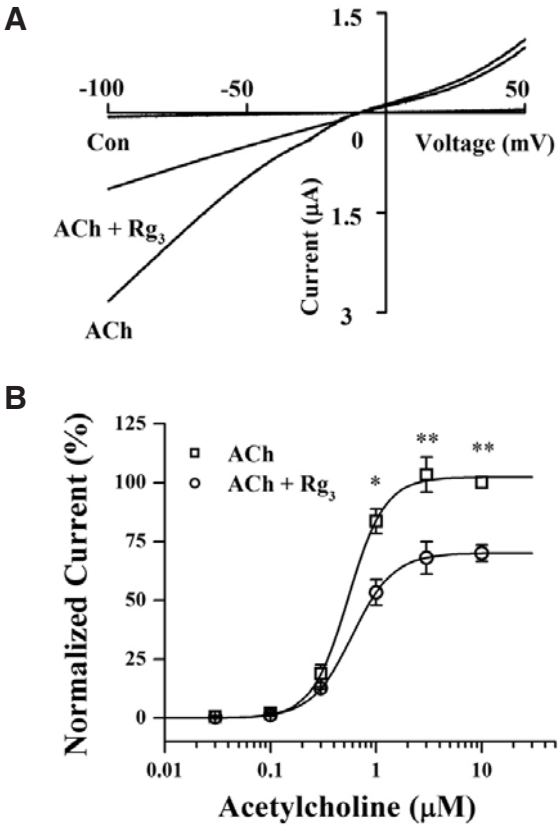

Fig. 4. Current-voltage relationship and non-competitive inhibition of L247T receptors. (A) Current-voltage relationships of I_{ACh} blockage by Rg_3 in wild-type or L247T receptors. Representative current-voltage relationships were obtained using voltage ramps of -100 to +50 mV for 300 ms at a holding potential of -80 mV. Voltage steps were applied before and after application of 0.5 μM acetylcholine in the absence or presence of 100 μM Rg_3. The reversal potential for the L247T receptors was not significantly different from that of the wild-type receptor in the absence or presence of Rg_3 (-10.4 ± 2.5 mV; with Rg_3, -11.5 ± 2.8 mV), but was linear rather than inward rectified (Revah et al., 1991). (B) Concentration-response relationships for acetylcholine in the L247T mutant receptor treated with acetylcholine (0.03-10 μM) alone or acetylcholine plus 100 μM Rg_3 in oocytes expressing the L247T receptor. The I_{ACh} of oocytes expressing the L247T mutant receptor was measured using the indicated concentrations of acetylcholine. The I_{ACh} of oocytes expressing the L247T mutant receptor was measured using the indicated concentration of acetylcholine in the absence (□) or presence (○) of 100 μM Rg_3. Oocytes were voltage-clamped at a holding potential of -80 mV. Oocytes were exposed to acetylcholine alone or acetylcholine plus Rg_3 for 30 s. Each point represents the mean ± S.E.M. (n = 9-12/group).

ingly, the best-fit docking results showed that Rg_3 forms three hydrogen bonds with L247T, but not with wild-type nAChRs (Fig. 6C). In L247T nAChRs, the first carbohydrate coupled to the Rg_3 backbone forms one hydrogen bond with Thr244 of subunit II, and the second carbohydrate of Rg_3 forms two hydrogen bonds with Ser240 of domain I and Thr244 of subunit V in the central pore (Fig. 6C). On the other hand, none of the 10 most likely docking sites demonstrated pore blockage of the wild-type channel by Rg_3. Instead, the Rg_3 binding site was located at the interface of two subunits of the wild-type channel (Fig. 6A). L247T, but not wild-type nAChR, allows Rg_3 to enter the channel pore and interact with several amino acids in the channel pore via hydrogen bond formation. Thus, from our virtual docking model it appears that Rg_3-mediated inhibition of I_{ACh} in L247T but not wild-type α7 nAChRs might be achieved by channel pore plugging activity of Rg_3.

DISCUSSION

The α7 AChR, which is a neuronal expressed receptor and is homomeric in composition, is widely expressed throughout the central nervous system including cortical and limbic areas and is known to play an important role in normal brain functions, as α7 AChR dysfunction is associated with neurological disorders such as Alzheimer's disease, schizophrenia, and epilepsy (Changeux and Edelstein, 2001; Chini et al., 1994; Lena and Changeux, 1997; Weiland et al., 2000). Recently, mutation of Leu247 to Thr247 in the TM2 pore region was found to decrease the rate of desensitization in response to acetylcholine, increase the apparent affinity for acetylcholine, and abolish current rectification, thus creating a gain-of-function activity for this receptor (Bertrand et al., 1992; Orr-Urtreger et al., 2000; Revah et al., 1991). In addition, homozygous mutation of the L250T α7 nAChR mutation (T/T) is lethal in mice, and heterozygous mice (+/T) show enhanced sensitivity to nicotine (Broide et al., 2002; Orr-Urtreger et al., 2000). These results indicate that the Leu247 residue in α7 nAChR plays a key role in maintaining homeostasis in the central nervous system.

In the present study, we demonstrated that (1) the mutant receptors L247A, L247D, L247E, L247I, L247S, and L247T, excluding L247K, caused a large leftward shift in acetylcholine concentration-response curves by 13.3-195.5-fold compared to the wild-type receptor (Fig. 1C), (2) co-application of Rg_3 and acetylcholine inhibited I_{ACh} in oocytes expressing chick L247A, L247D, L247E, L247I, or L247S, but not in oocytes expressing wild-type or L247K α7 nAChRs, in a reversible and concentration-dependent manner, (3) inhibition of I_{ACh} by Rg_3 occurred in a non-competitive and voltage-dependent manner in oocytes expressing L247T α7 nAChRs, (4) a virtual modeling technique allowed us to explain how Rg_3 exhibits its inhibitory effects on I_{ACh} in the L247T mutant, but not the wild-type receptor (Fig. 6).

In addition, we investigated the mechanism by which Rg_3 inhibits L247T α7 nAChRs by measuring the effect of 100 μM Rg_3 on different concentrations of ACh for α7 L247T receptors. Concentration-response curves obtained in the absence of Rg_3 were similar to those reported previously for other nAChR subtypes (Choi et al., 2002; Sala et al., 2002). In the presence of Rg_3, a negligible shift in the ACh dose-response curve was obtained, and current inhibition was not relieved even at high acetylcholine concentrations. Thus, Rg_3-mediated inhibition of I_{ACh} in L247T α7 nAChRs was maintained at 3 to 10 μM acetylcholine concentrations. These results support a noncompetitive mechanism by which Rg_3 is involved in L247T α7 nAChR regulation. Thus, Rg_3 interaction sites with nAChRs are differ from those of acetylcholine.

Based on the present results, we also found that Rg_3 inhibits I_{ACh} via a membrane holding potential-dependent manner in oocytes expressing L247T α7 nAChR. In other words, Rg_3-mediated inhibition of I_{ACh} was greatly attenuated at more depolarizing potentials. These results raise the possibility that Rg_3 may act as an open channel blocker of L247T α7 nAChRs, despite lacking a charged group. Open channel blockers such as local anesthetics or hexamethonium are strongly voltage dependent due to the charge that they carry in the transmembrane electrical field (Arias, 1996; Heidmann et al., 1983; Sine

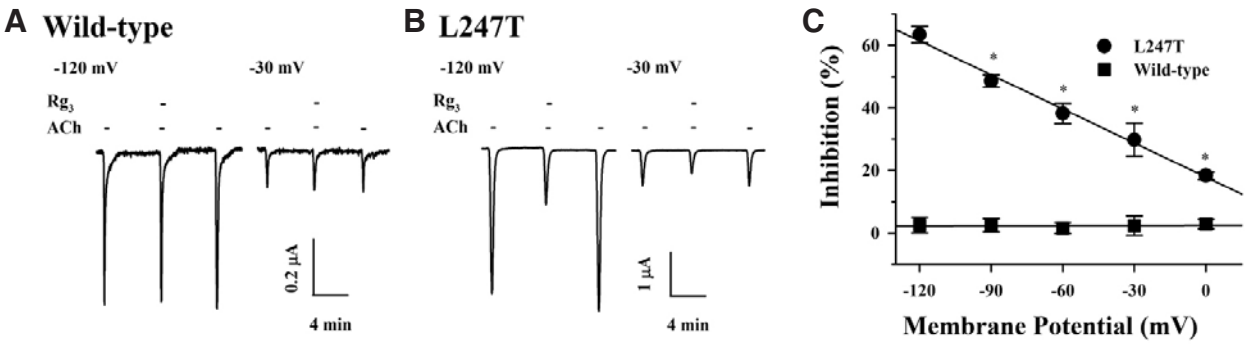

Fig. 5. Voltage-dependent inhibition of L247T receptors by Rg_3. (A, B) The representative traces were obtained from wild-type and L247T receptors in the absence or presence of Rg_3. (C) Summary of percent inhibition induced by Rg_3 at the indicated membrane holding potentials in oocytes expressing wild-type or mutant α7 receptor. *$p < 0.005$, compared to -120 mV membrane holding potential. Each point represents the mean ± S.E.M. (n = 9-12/group).

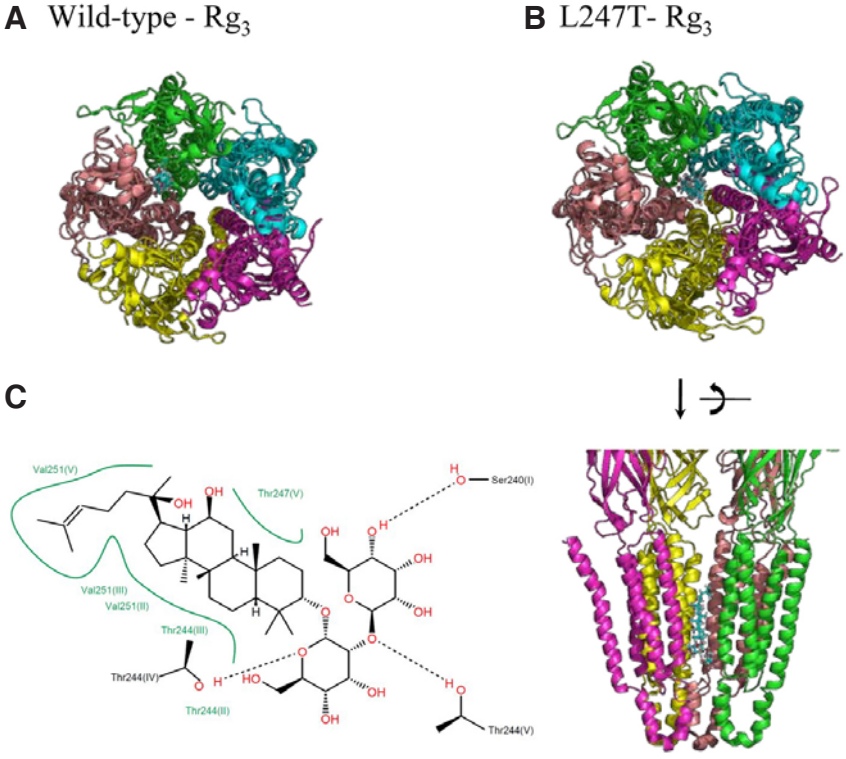

Fig. 6. Virtual dockings of Rg_3 to chick wild-type and L247T α7 nAChR channel homology models. (A) Top view of the highest-ranked docking model of Rg_3 to the wild-type channel. The channel is shown as a cartoon diagram and Rg_3 is indicated as a ball and chain model. Each subunit is shown in different colors. (B) Top view and side view of the highest-ranked docking model of Rg_3 to the L247T receptor. One of the subunits is omitted in the side view for clarity. All of the top 10 docking results displayed pore blocking of the mutant channel by Rg_3. (C) Poseview analysis of protein-ligand interactions. Hydrogen bonding is denoted by a dotted line. The spline sections indicate hydrophobic contacts, highlighting the hydrophobic regions of Rg_3 and the identity of the contacting amino acid. The roman numerals in parenthesis indicate each subunit of the pentamer.

and Tayler, 1982). Similarly, in our previous report, we also demonstrated that Rg_3 inhibits inward cation currents through the open state of the V291A 5-HT_{3A} receptor, which exhibits constitutively active ion currents (Lee et al., 2007). These results suggest that Rg_3 acts as a non-charged open channel blocker of cation ligand-gated ion channels.

The second transmembrane domain (TM2) lines the wall of the pore. The Leu residue corresponding to position 247 of the chick α7 nAChR channel is highly conserved in all nicotinic, $GABA_A$, 5-HT_3 and glycine receptors, and has been believed to be positioned at the gate (Lester et al., 2004). Recently acquired high resolution structures of the *Torpedo* nAChR channel show that the conserved Leu, is located at the narrowest part of the channel, and the side chain of the amino acid head point toward to the lumen of the pore (Miyazawa et al., 2003; Unwin, 2005). The importance of position 247 for gating and conductance has also been demonstrated in a functional study (Bertrand et al., 1992; Palma et al., 1996; Revah et al., 1991). The homology modeling and virtual docking used in the present study provide insight into the mechanism by which Rg_3 exerts its inhibitory effect on L247T receptors. Exchange of the larger amino acid, leucine, present in the wild-type receptor for the smaller amino acid, threonine, at position 247 might cause conformational changes in the mutant receptor subunits following acetylcholine binding and induce opening of the channel pore (Lyford et al., 2003). In this state, the mutant receptor might allow for tight plugging of the Rg_3 molecule via formation of hydrogen bonds with amino acids in the aqueous pore, an impossibility in the wild-type receptor due to steric hindrance (Fig. 6A). Thus, the channel pore plugging action of Rg_3 in the L247T receptor might cause voltage-dependent and non-competitive blockage of ion currents following receptor activation.

As mentioned above, although α7 nACh and 5-HT_{3A} are both homomeric ligand-gated ion channels and share many amino acid sequence homologies in TM2 (Fig. 1B), Rg_3-mediated regulation differs considerably between these two receptors; Rg_3 exhibits an inhibitory effect on the wild-type 5-HT_{3A} receptor, but has no effect on the wild-type α7 nAChR. The F292A mutation in TM2 of homomeric 5-HT_{3A} receptors abolishes Rg_3-induced inhibition of peak $I_{5\text{-}HT}$ (Lee et al., 2007), whereas the L247A, L247D, L247E, L247I, L247S and L247T but not F252A mutations in α7 nAChR sensitized the mutant receptors to Rg_3 (Fig. 2D). In addition, when we examined the effects of Rg_3 on I_{ACh} after double mutations (L247T-F292A) of amino acids including homologous to that present in the 5-HT_{3A} receptor (Fig. 1B), we could not observe the any changes of Rg_3-induced inhibitions of I_{ACh} (data not shown). These results show a possibility that Rg_3 interaction sites in L247T α7 nAChR and wild-type 5-HT_{3A} receptors are not topologically similar. However, the L247T α7 receptor provides additional evidence that Rg_3 interacts with amino acids in TM2 to regulate cation ligand-gated ion channels. Currently, we do not understand why co-application of Rg_3 and acetylcholine inhibited I_{ACh} in oocytes expressing chick L247A, L247D, L247E, L247I, L247S or L247T but not in oocytes expressing wild-type or L247K α7 nAChRs. Further study might be required to elucidate the relationships between characteristics of amino acid and sensitivity to Rg_3.

In summary, we found that, although Rg_3 had no effect on I_{ACh} in oocytes expressing chick wild-type α7 nAChRs, site-directed mutation of Leu247 to other amino acid residues rendered the receptor sensitive to Rg_3. The inhibitory effect of Rg_3 on I_{ACh} in L247T receptors was non-competitive and voltage-dependent. Homology modeling and virtual docking show that Rg_3 might inhibit L247T receptor channel currents by plugging the channel pore. This result might provide an advance in understanding of pharmacological effects of *Panax ginseng*.

ACKNOWLEDGMENTS

This work was supported by grants provided to S.Y. Nah from the Brain Korea 21 project, the Korea Science and Engineering Foundation funded by the Ministry of Education, Science and Technology (R01-2008-000-10448-0), a grant to H. Choe from Asan Institute for Life Sciences (2008-307), and by a grant given to H. Rhim from the Korea Institute of Science and Technology Core-Competence Program funded by the Ministry of Education, Science and Technology.

REFERENCES

Arias, H.R. (1996). Luminal and non-luminal non-competitive inhibitor binding sites on the nicotinic acetylcholine receptor. Mol. Membr. Biol. *13*, 1-17.

Bertrand, D., Devillers-Thiery, A., Revah, F., Galzi, J.L., Hussy, N., Mulle, C., Bertrand, S., Ballivet, M., and Changeux, J.P. (1992). Unconventional pharmacology of a neuronal nicotinic receptor mutated in the channel domain. Proc. Natl. Acad. Sci. USA *89*, 1261-1265.

Boulter, J., Evans, K., Goldman, D., Martin, G., Treco, D., Heinemann, S., and Patrick, J. (1986). Isolation of a cDNA clone coding for a possible neural nicotinic acetylcholine receptor alpha-subunit. Nature *319*, 368-374.

Boulter, J., Connolly, J., Deneris, E., Goldman, D., Heinemann, S., and Patrick, J. (1987). Functional expression of two neuronal nicotinic acetylcholine receptors from cDNA clones identifies a gene family. Proc. Natl. Acad. Sci. USA *84*, 7763-7767.

Broide, R.S., Salas, R., Ji, D., Paylor, R., Patrick, J.W., Dani, J.A., and De Biasi, M. (2002). Increased sensitivity to nicotine-induced seizures in mice expressing the L250T alpha7 nicotinic acetylcholine receptor mutation. Mol. Pharmacol. *61*, 695-705.

Bryson, K., McGuffin, L.J., Marsden, R.L., Ward, J.J., Sodhi, J.S., and Jones, D.T. (2005). Protein structure prediction servers at University College London. Nucleic Acids Res. *33*, W36-38.

Castro, N.G., and Albuquerque, E.X. (1995). alpha-Bungarotoxin-sensitive hippocampal nicotinic receptor channel has a high calcium permeability. Biophys. J. *68*, 516-24.

Changeux, J.P., and Edelstein, S.J. (2001). Allosteric mechanisms in normal and pathological nicotinic acetylcholine receptors. Curr. Opin. Neurobiol. *11*, 369-377.

Chini, B., Raimond, E., Elgoyhen, A.B., Moralli, D., Balzaretti M., and Heinemann, M. (1994). Molecular cloning and chromosomal localization of the human alpha 7-nicotinic receptor subunit gene (CHRNA7). Genomics *19*, 379-381.

Choi, S., Jung, S.Y., Lee, J.H., Sala, F., Criado, M., Mulet, J., Valor, L.M., Sala, S., Engel, A.G., and Nah, S.Y. (2002). Effects of ginsenosides, active components of ginseng, on nicotinic acetylcholine receptors expressed in Xenopus oocytes. Eur. J. Pharmacol. *442*, 37-45.

Couturier, S., Bertrand, D., Matter, J.M., Hernandez, M.C., Bertrand, S., Millar, N., Valera, S., Barkas, T., and Ballivet, M. (1990). A neuronal nicotinic acetylcholine receptor subunit (α7) is developmentally regulated and forms a homooligomeric channel blocked by α-BTX. Neuron *5*, 847-856.

Elgoyhen, A.B., Johnson, D.S., Boulter, J., Vetter, D.E., and Heinemann, S. (1994). α9: an acetylcholine receptor with novel pharmacological properties expressed in rat cochlear hair cells. Cell *79*, 705-715.

Gotti, C., and Clementi, F. (2004) Neuronal nicotinic receptors: from structure to pathology. Prog. Neurobiol. *74*, 363-396.

Gotti, C., Hanke, W., Maury, K., Moretti, M., Ballivet, M., Clementi, F., and Bertrand, D. (1994). Pharmacology and biophysical properties of α7 and α7-α8 α-bungarotoxin receptor subtypes immunopurified from the chick optic lobe. Eur. J. Neurosci. *6*, 1281-1291.

Gotti, C., Carbonnelle, E., Moretti, M., Zwart, R., and Clementi, F. (2000). Drugs selective for nicotinic receptor subtypes: a real possibility or a dream? Behav. Brain Res. *113*, 183-192.

Heidmann, T., Oswald, R.E., and Changeux, J.P. (1983). Multiple sites of action for noncompetitive blockers on acetylcholine receptor rich membrane fragments from torpedo marmorata. Biochemistry *22*, 3112-3127.

Jensen, M.L., Schousboe, A., and Ahring, P.K. (2005). Charge selectivity of the Cys-loop family of ligand-gated ion channels. J. Neurochem. *92*, 217-225.

Karlin, A. (2002). Emerging structure of the nicotinic acetylcholine receptors. Nat. Rev. Neurosci. *3*, 102-114.

Krogh, A., Larsson, B., von Heijne, G., and Sonnhammer, E.L. (2001). Predicting transmembrane protein topology with a hidden Markov model: application to complete genomes. J. Mol. Biol. *305*, 567-580.

Le Novère, N., and Changeux, J.P. (1995). Molecular evolution of the nicotinic acetylcholine receptor: an example of multigene family in excitable cells. J. Mol. Evol. *40*, 155-172.

Lee, J.H., Jeong, S.M., Kim, J.H., Lee, B.H., Yoon, I.S., Lee, J.H., Choi, S.H., Kim, D.H., Rhim, H., Kim, S.S., et al. (2005). Characteristics of ginsenoside Rg_3-mediated brain Na^+ current inhibition. Mol. Pharmacol. *68*, 1114-1126.

Lee, B.H., Lee, J.H., Lee, S.M., Jeong, S.M., Yoon, I.S., Lee, J.H., Choi, S.H., Pyo, M.K., Rhim, H., Kim, H.C., et al. (2007). Identification of ginsenoside interaction sites in 5-HT_{3A} receptors. Neuropharmacology *52*, 1139-1150.

Lena, C., and Changeux, J.P. (1997). Pathological mutations of nicotinic receptors and nicotine-based therapies for brain disorders. Curr. Opin. Neurobiol. *7*, 674-682.

Lester, H.A., Dibas, M.I., Dahan, D.S., Leite, J.F., and Dougherty, D.A. (2004). Cys-loop receptors: new twists and turns. Trends Neurosci. *27*, 329-336.

Lyford, L.K., Sproul, A.D., Eddins, D., McLaughlin, J.T., and Rosenberg, R.L. (2003). Agonist-induced conformational changes in the extracellular domain of alpha 7 nicotinic acetylcholine receptors. Mol. Pharmacol. *64*, 650-658.

Miyazawa, A., Fujiyoshi, Y., and Unwin, N. (2003). Structure and gating mechanism of the acetylcholine receptor pore. Nature *42*, 949-955.

Nah, S.Y., Kim, D.H., and Rhim, H. (2007). Ginsenosides: are any of them candidates for drugs acting on the central nervous system? CNS Drug Rev. *13*, 381-404.

Nashmi, R., and Lester, H.A. (2006). CNS localization of neuronal nicotinic receptors. J. Mol. Neurosci. *30*, 181-184.
Orr-Urtreger, A., Broide, R.S., Kasten, M.R., Dang, H., Dani, J.A., Beaudet, A.L., and Patrick, J.W. (2000). Mice homozygous for the L250T mutation in the alpha7 nicotinic acetylcholine receptor show increased neuronal apoptosis and die within 1 day of birth. J. Neurochem. *74*, 2154-2166.
Palma, E., Mileo, A.M., Eusebi, F., and Miledi, R. (1996). Threonine-for-leucine mutation within domain M2 of the neuronal α7 nicotinic receptor converts 5-hydroxytryptamine from antagonist to agonist. Proc. Natl. Acad. Sci. USA *93*, 11231-11235
Revah, F., Bertrand, D., Galzi, J.L., Devillers-Thiéry, A., Mulle, C., Hussy, N., Bertrand, S., Ballivet, M., and Changeux, J.P. (1991). Mutations in the channel domain alter desensitization of a neuronal nicotinic receptor. Nature *353*, 846-849.
Sala, F., Mulet, J., Choi, S., Jung, S.Y., Nah, S.Y., Rhim, H., Valor, L.M., Criado, M., and Sala, S. (2002). Effects of ginsenoside Rg_2 on human neuronal nicotinic acetylcholine receptors. J. Pharmacol. Exp. Ther. *301*, 1052-1059.
Sali, A., and Blundell, T.L. (1993). Comparative protein modelling by satisfaction of spatial restraints. J. Mol. Biol. *234*, 779-815.
Séguéla, P., Wadiche, J., Dineley-Miller, K., Dani, J.A., and Patrick, J.W. (1993). Molecular cloning, functional properties, and distribution of rat brain alpha 7: a nicotinic cation channel highly permeable to calcium. J. Neurosci. *13*, 596-604.
Sine, S.M., and Taylor, P. (1982). Local anesthetics and histrionicotoxin are allosteric inhibitors of the acetylcholine receptor. Studies of clonal muscle cells. J. Biol. Chem. *257*, 8106-8114.
Stierand, K., Maass, P.C., and Rarey, M. (2006). Molecular complexes at a glance: automated generation of two-dimensional complex diagrams. Bioinformatics *22*, 1710-1716.
Unwin, N. (2005). Refined structure of the nicotinic acetylcholine receptor at 4A resolution. J. Mol. Biol. *346*, 967-989.
Verdonk, M.L., Cole, J.C., Hartshorn, M.J., Murray, C.W., and Taylor, R.D. (2003). Improved protein-ligand docking using GOLD. Proteins *52*, 609-623.
Weiland, S., Bertrand, D., and Leonard, S. (2000). Neuronal nicotinic acetylcholine receptors: from the gene to the disease. Behav. Brain Res. *113*, 43-56.